CrossMark

ORIGINAL ARTICLE

Homogenous–heterogeneous reactions in MHD flow of Powell–Eyring fluid over a stretching sheet with Newtonian heating

Imad Khan[1] · M. Y. Malik[1] · T. Salahuddin[2] · Mair Khan[1] · Khalil Ur Rehman[1,2]

Abstract This article addresses the effects of homogenous–heterogeneous reactions on electrically conducting boundary layer fluid flow and heat transfer characteristics over a stretching sheet with Newtonian heating are examined. Using similarity transformations, the governing equations are transformed into nonlinear ordinary differential equations. The constricted ordinary differential equations are solved computationally by shooting technique. The impact of pertinent physical parameters on the velocity, concentration and temperature profiles is discussed and explored via figures and tables. It is clear from figures that the velocity profile reduces for large values of fluid parameter B and Hartmann number H. Skin friction coefficient decreases for large values of Hartmann number H and fluid parameter B. Also, heat transfer rate monotonically enhances with conjugate parameter of Newtonian heating γ and Prandtl number Pr.

Keywords Powell–Eyring fluid model · Homogenous–heterogeneous reactions · Stretching sheet · Newtonian heating

1 Introduction

Fluids used in industries maximum are non-Newtonian in nature which do not have a direct relationship between stress and deformation rate, e.g., molten polymers, biological fluids, lubricants, mud and some fluids occurring naturally such as animal blood. These fluids have been distributed into different classes. Among these, one of the important models is Powell–Eyring fluid model which is many beneficial over the other non-Newtonian models, i.e., power law, Maxwell and micropolar fluid models. Although the considered model is very intricate and has favorite over the other fluid models, power law model is induced rather than the empirical relation from kinetic theory of liquid. It condenses to Newtonian relevance at high and low shear rates. Recently, the Powell–Eyring fluid was numerically studied by Akbar et al. [1]. They revealed the impact on Powell–Eyring due to magnetic field on Powell–Eyring fluid over a stretching surface. They analyzed that the velocity profile fell down with intensity enhancement of the magnetic flux and Powell–Eyring fluid parameters. Malik et al. [2] analyzed the flow of Powell–Eyring fluid above a stretching cylinder and considered two models, namely Reynaldo's and Vogel's models. They observed that boundary layer reduced for large Prandtl number values. Also, they analyzed that velocity profile increased by enhancing the values of suction parameter. The temperature profile reduces for large values of suction parameter. Ara et al. [3] illustrated the flow of Powell–Eyring fluid exponentially over a shrinking surface. They examined that velocity profile increased with the mass suction increment, while temperature profile showed opposite behavior. Also, the boundary layer thickness reduced with increase in Prandtl number. Nadeem and Saleem [4] observed the free and force convection flow by

✉ Imad Khan
  imadkhan@math.qau.edu.pk

1 Department of Mathematics, Quaid-i-Azam University, Islamabad 44000, Pakistan

2 Mirpur University of Science and Technology (MUST), Mirpur, Pakistan

 Springer

a stretching cone in the existence of mass and heat transfer. They observed that tangential velocity has opposite behavior for flow parameters. Moreover, they observed that skin friction coefficient increased due to the increment in ratio of buoyancy forces to flow parameter. Hayat et al. [5] examined the comparison of series and numerical solutions for flow of Powell–Eyring fluid with Newtonian heating. Also, they considered the internal heat generation and absorption. Malik et al. [6] used Keller box method and analyzed the MHD flow of tangent hyperbolic fluid over a stretching cylinder. Also in Refs. [7–10], authors investigated the Powell–Eyring fluid model in different physical conditions.

The heterogeneous and homogenous reactions are natural processes of chemical reactions. Several reactions progress very slowly, without a catalyst. The natural processes of heterogeneous and homogenous reactions are actually very complex including the consumption and production of reactant species at various rates on both the catalyst surface and fluid, i.e., reactions occurring in biochemical system, combustion and catalysis. Merkin [11] investigated the homogeneous and heterogeneous reactions for isothermal boundary layer flow model. Sarif et al. [12] have reported numerically the behavior of heat transfer past over a stretching plate. They demonstrated that boundary layer thickness varied with Prandtl number. Also, they investigated that temperature profile reduced by enhancement of Prandtl number and conjugate parameter. Kameswaran et al. [13] described the disintegration of the boundary layer flow past over a stretching surface with homogenous and heterogeneous reactions. They analyzed that velocity profile reduced with enhancement of concentration profile. Also, they observed that skin friction coefficient enhanced with increase in porous permeability parameter. They found that concentration reduced with the strength of heterogeneous reactions. Shaw et al. [14] examined the homogenous and heterogeneous reactions on the micropolar fluid flow and assumed porous stretching/shrinking sheet. They analyzed that momentum boundary layer thickness enhanced in the case of stretching sheet and fell down in the case of shrinking surface. Also, concentration profile has same results in the case of stretching/shrinking surface. They illustrated that the concentration reduced with the strength of the homogenous and heterogeneous reactions. The concentration of the reaction and fluid velocity on the surface increased with increase in stretching/shrinking parameters, while velocity enhanced with enhancement of micropolar parameter. The strength of homogenous and heterogeneous reactions reduces the strength of concentration reactants. Abbas et al. [15] observed the impacts of homogenous and heterogeneous reactions with stagnation point over a porous shrinking/stretching surface in attendance of transverse magnetic field. They observed that concentration of boundary layer thickness reduced by

enhancing the suction and magnetic parameters in the case of stretching plate, but revealed increasing behavior for shrinking sheet case. Ellahi et al. [16] examined the characteristic effects of mixed convection MHD nanofluid over a vertical stretching surface. They noticed that velocity enhanced by enhancing the chemical dimensions and the radius of the gyration. References [17, 18] elaborate the recent work related to homogenous and heterogeneous reactions.

Flow generated by a shrinking/stretching surface produces a great interest due to several applications in industries and engineering, e.g., two-dimensional steady flow is used for contracting and expanding the surface such as stretching/shrinking wrapping bundle, aluminum bottle industrial procedures, wrapping and hot rolling. These flows with heat transfer have a great importance in paper production, enhanced petroleum resources, food processing, etc. Nadeem et al. [19, 20] analyzed the boundary layer flow with point of stagnation. They observed that velocity field enhanced with enhancement of local injection and suction parameter. Akbar et al. [21] numerically analyzed the boundary layer flow of hyperbolic tangent fluid over a stretching surface. They analyzed that velocity profile reduced with increasing Hartmann number, while similar phenomena were noticed for velocity profile in power law index. They observed that Weissenberg number reduced the velocity profile. Also, they observed that increasing the Weissenberg number and power law increased the skin friction coefficient. Malik et al. [22] reported the flow of boundary layer over exponentially stretching cylinder. They illustrated that by enhancing the values of Casson fluid parameter velocity profile fell down while velocity profile increased by enhancing the mixed convection parameter. Also, they discussed that temperature profile fell down by enhancing the Reynolds number and Prandtl number. Tain et al. [23] observed the transfer of heat and fluid flow over a stretching plate with MHD and temperature-dependent viscosity. They analyzed that enhancement of Prandtl number decreases thermal boundary layer thickness. Lee [24] studied the boundary layer from smooth to rough surface with a step change. Zeeshan et al. [25] studied the effects of magnetic dipole on viscous ferrofluid past over a stretching surface with thermal radiation. Recent work on boundary layer flow and transfer of heat is mentioned in Refs. [18, 26–31].

The main motivations of this analysis are to analyze the effects of MHD flow of electrically conducting Powell–Eyring fluid over a stretching plate and also consider Newtonian heating with heterogeneous and homogenous reactions. The nonlinear expression concentration is transformed into ordinary differential expressions, and then, shooting method is employed in computing the result in MATLAB package. Numerical results are explained with tables and graphs.

2 Method of solution

Consider incompressible two-dimensional steady flow of non-Newtonian fluid over a stretching surface with homogenous and heterogeneous reactions. The sheet is suddenly stretched such that the fluid flow with velocity $u_w = cx$, where c is a nonnegative constant. Consider two-dimensional coordinates system such that x is taken along with the plate, while the y-axis is taken at right angle to the sheet. We assume interaction between homogenous and heterogeneous reaction for a small model. Mathematical form of these reactions is given as:

$$A + 2B \rightarrow 3B, \text{ rate} = K_c ab^2, \tag{1}$$

$$A \rightarrow B, \text{ rate} = K_s a. \tag{2}$$
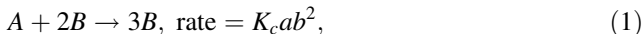
In the above equations, b and a are the concentration of chemical species B and A and Ki ($i = s, c$) are the rate constant. The stream function ψ such that $u = \frac{\partial \psi}{\partial y}$ and $v = -\frac{\partial \psi}{\partial y}$ identically satisfies the continuity equation. All the governing laws are mathematically given as:

$$\frac{\partial v}{\partial y} + \frac{\partial u}{\partial x} = 0, \tag{3}$$

$$
\begin{aligned}
u\frac{\partial u}{\partial x} + v\frac{\partial u}{\partial y} \\
= \left(v + \frac{1}{\rho\beta c}\right)\left(\frac{\partial^2 u}{\partial x^2} + \frac{\partial^2 u}{\partial y^2}\right) \\
- \frac{1}{3\rho\beta c^3}\frac{\partial}{\partial x}\left\{2\left(\frac{\partial v}{\partial y}\right)^2 + \left(\frac{\partial u}{\partial y} + \frac{\partial v}{\partial x}\right)^2 + 2\left(\frac{\partial u}{\partial x}\right)^2\right\}\frac{\partial u}{\partial x} \\
- \frac{1}{6\rho\beta c^3}\frac{\partial}{\partial y}\left\{2\left(\frac{\partial v}{\partial y}\right)^2 + \left(\frac{\partial u}{\partial y} + \frac{\partial v}{\partial x}\right)^2 + 2\left(\frac{\partial u}{\partial x}\right)^2\right\}\left(\frac{\partial u}{\partial y} + \frac{\partial v}{\partial x}\right) - \frac{\sigma B^2 u}{\rho},
\end{aligned} \tag{4}
$$

$$
\begin{aligned}
u\frac{\partial v}{\partial x} + v\frac{\partial v}{\partial y} \\
= \left(v + \frac{1}{\rho\beta c}\right)\left(\frac{\partial^2 v}{\partial x^2} + \frac{\partial^2 v}{\partial y^2}\right) \\
- \frac{1}{6\rho\beta c^3}\frac{\partial}{\partial x}\left\{2\left(\frac{\partial v}{\partial y}\right)^2 + \left(\frac{\partial u}{\partial y} + \frac{\partial v}{\partial x}\right)^2 + 2\left(\frac{\partial u}{\partial x}\right)^2\right\}\left(\frac{\partial u}{\partial y} + \frac{\partial v}{\partial x}\right) \\
- \frac{1}{3\rho\beta c^3}\frac{\partial}{\partial y}\left\{2\left(\frac{\partial u}{\partial x}\right)^2 + \left(\frac{\partial u}{\partial y} + \frac{\partial v}{\partial x}\right)^2 + 2\left(\frac{\partial v}{\partial y}\right)^2\right\}\frac{\partial v}{\partial y},
\end{aligned} \tag{5}
$$

$$
\begin{aligned}
u\frac{\partial T}{\partial x} + v\frac{\partial T}{\partial y} \\
= \alpha\left(\frac{\partial^2 T}{\partial y^2} + \frac{\partial^2 T}{\partial x^2}\right) + \tau\left\{D_B\left(\frac{\partial C}{\partial x}\frac{\partial T}{\partial x} + \frac{\partial C}{\partial y}\frac{\partial T}{\partial y}\right)\right. \\
\left. + \left(\frac{D_T}{T_\infty}\right)\left[\left(\frac{\partial T}{\partial x}\right)^2 + \left(\frac{\partial T}{\partial y}\right)^2\right]\right\},
\end{aligned} \tag{6}
$$

$$u\frac{\partial a}{\partial x} + v\frac{\partial a}{\partial y} = D_A\frac{\partial^2 a}{\partial y^2} - k_c ab^2, \tag{7}$$

$$u\frac{\partial b}{\partial x} + v\frac{\partial b}{\partial y} = D_B\frac{\partial^2 b}{\partial y^2} + k_c ab^2, \tag{8}$$

and the associated boundary conditions are as follows:

$$u = u_w(x) = cx, \quad \frac{\partial T}{\partial y} = -h_s T, \quad v = 0, \quad \text{at } y = 0,$$

$$T \rightarrow T_\infty, \quad u \rightarrow 0, \quad \text{as } y \rightarrow \infty,$$

$$D_B\left(\frac{\partial b}{\partial y}\right)_{y=0} = -k_s a(0), \quad D_A\left(\frac{\partial a}{\partial y}\right)_{y=0} = k_s a(0),$$

$$u(\infty) = u_e(x), \quad a(\infty) = a_0, \quad b(\infty) = 0. \tag{9}$$

In the above equations, v and u are the components of velocity in the y- and x-directions, respectively. μ is the dynamic viscosity, $v = \frac{\mu}{\rho}$ is the kinematic viscosity, ρ is the density, β is the fluid parameter, σ is the electrical conductivity of the fluid, H is the strength of magnetic field, α is the thermal diffusivity, for Newtonian heating h_s is the heat transfer parameter and τ is the ratio of heat capacity and effective heat capacity of the fluid. After applying the boundary layer approximation in Eqs. (3)–(8), we get the following formulas:

$$u\frac{\partial u}{\partial x} + v\frac{\partial u}{\partial y} = \left(v + \frac{1}{\rho\beta c}\right)\left(\frac{\partial^2 u}{\partial y^2}\right) - \frac{1}{2\rho\beta c^3}\left(\frac{\partial u}{\partial y}\right)^2\frac{\partial^2 u}{\partial y^2} - \frac{\sigma u B^2}{\rho}, \tag{10}$$

$$u\frac{\partial T}{\partial x} + v\frac{\partial T}{\partial y} = \alpha\left(\frac{\partial^2 T}{\partial y^2}\right) + \tau\left\{D_B\left(\frac{\partial T}{\partial x}\frac{\partial C}{\partial x}\right) + \frac{D_T}{T_\infty}\left(\frac{\partial T}{\partial x}\right)^2\right\}, \tag{11}$$

$$u\frac{\partial a}{\partial x} + v\frac{\partial a}{\partial y} = D_A\frac{\partial^2 a}{\partial y^2} - k_c ab^2, \tag{12}$$

$$u\frac{\partial b}{\partial x} + v\frac{\partial b}{\partial y} = D_B\frac{\partial^2 b}{\partial y^2} + k_c ab^2. \tag{13}$$

The similarity transformations are defined as:

$$\Psi = (cv)^{\frac{1}{2}}xf(\eta), \quad \eta = \left(\frac{c}{v}\right)^{\frac{1}{2}}y, \quad u = cxf'(\eta), \quad \theta(\eta) = \frac{T - T_\infty}{T_w - T_\infty},$$

$$v = -\sqrt{cv}f(\eta), \quad g(\eta) = \frac{a}{a_0}, \quad h(\eta) = \frac{b}{a_0}, \tag{14}$$

where Ψ is the stream function, and by using these similarity transformations, Eqs. (10)–(13) become

$$(1 + M)f''' - f'^2 + ff'' - MBf''^2 f''' - Hf' = 0, \tag{15}$$

$$\theta'' + f Pr\, \theta' = 0, \tag{16}$$

$$\frac{1}{Sc}g'' + fg'^2 = 0, \tag{17}$$

$$\frac{\delta}{Sc}h'' + fh'^2 = 0, \tag{18}$$

transformed conditions are as follows:

$$f(0) = 0, \; f'(0) = 1, \; f'(\infty) \to 0, \; \theta(0) = \frac{\theta'(0)}{\gamma} + 1, \; \theta(\infty) \to 0,$$

$$g'(0) = K_s g(0), \; g(\infty) = 1,$$

$$(19)$$

and suppose further that diffusion coefficient D_B and D_A are equal, i.e., $\delta = 1$, and by using these assumptions, following relation is obtained:

$$g(\eta) + h(\eta) = 1, \tag{20}$$

and by using Eq. (20), Eqs. (17) and (18) become

$$\frac{1}{Sc} g'' + fg'^2 = 0, \tag{21}$$

with associated conditions

$$g(\infty) = 1 \; g'(0) = K_s g(0) \tag{22}$$

In the above mathematical equations, prime denotes the differentiation w.r.t. η. $Pr = \frac{\nu}{\alpha}$ denoted the Prandtl number, $H = \frac{\sigma B^2}{\rho}$ is the Hartmann number, $M = \frac{1}{\mu\beta c}$ and $B = \frac{a^3 x^2}{2C^2 \nu}$ are fluid parameters, $K = \frac{k_c a_0^2}{c}$ is the measure of the strength of the homogenous reaction, $Sc = \frac{\nu}{D_A}$ is the Schmidt number, $\delta = \left(\frac{D_B}{D_A} \right)$ is the ratio of the coefficient of diffusion, $\gamma = \frac{h_s}{\left(\frac{c}{\nu}\right)^{\frac{1}{2}}}$ is the conjugate parameter for Newtonian heating, T_∞ is the free stream and T is the fluid temperature, respectively. The quantity of practical interest such as skin friction coefficient is defined as:

$$C_f = \frac{\tau_w}{\frac{1}{2}\rho u^2}, \; Nu = \frac{x q_w}{k(T_w - T_\infty)}, \tag{23}$$

where

$$\tau_w = \left[\left(1 + \frac{1}{\beta c} \right) \frac{du}{dy} - \frac{1}{6\beta c^3} \left(\frac{\partial u}{\partial y} \right)^3 \right],$$

and

$$(24)$$

$$q_w = -K \frac{\partial T}{\partial y} \Big|_{y=0},$$

and the coefficient of skin friction and heat transfer coefficient become:

$$C_f Re x^{\frac{1}{2}} = \left[(1 + M) f''(0) - \frac{\lambda}{3} f''^3(0) \right] Nu Re x^{\frac{1}{2}} = -\theta'(0). \tag{25}$$

2.1 Numerical solution

Equations (15)–(18) along with the associated boundary condition (19) are solved numerically by using shooting method. First we convert this system of equations into the system of first-order initial value problem and then solve this problem by using shooting method. Suppose

$$f = h_1, \; f' = h_2, \; f'' = h_3, \; \theta = h_4, \; \theta' = h_5, \; g = h_6, \; g' = h_7. \tag{26}$$

We get the system of ODEs

$$h_1' = h_2, \tag{27}$$

$$h_2' = h_3, \tag{28}$$

$$h_3' = \frac{1}{1 + M - MB h_3^2} \left[h_2^2 - h_1 h_3 + H h_2 \right], \tag{29}$$

$$h_4' = h_5, \tag{30}$$

$$h_5' = -Pr(h_1 h_5), \tag{31}$$

$$h_6' = h_7, \tag{32}$$

$$h_7' = Sc \left[K h_6 (1 - h_6)^2 - h_1 h_7 \right], \tag{33}$$

with transformed initial conditions

$$h_1(0) = 0, \; h_2(0) = 1, \; h_2(\infty) = 0, \; h_4(0) = 1, \; h_4(\infty) = 0, \; h_6(0) = 0, \; h_6(\infty) = 0, \; h_7(0) = K_s h_6(0). \tag{34}$$

Choose a suitable initial approximations for h_3 (0), h_5 (0) and h_7 (0) as 1, −1 and 1, respectively. Then, the system of first-order ODEs is solved using Runge–Kutta fifth-order technique. The convergence criterion for shooting method is 10^{-6} which absolute value of given and computed values of h_2, h_4 and h_6. Thus, if the error tolerance, i.e., 10^{-6}, is less than boundary residuals, then re-adjust initial guesses by Newton's method. This loop is recycled again until the required criteria are satisfied.

3 Results and discussion

The impact of certain flow parameters on concentration, temperature and velocity profiles is visualized in this section. Figure 1a shows the impact of Hartmann number H on velocity profile. It is examined that by enhancing the Hartmann number H the velocity profile decreases. This is due to the retarding nature of the Lorentz forces which reduces the motion of the fluid in the boundary layer and enhances its temperature. Figure 1b shows the impact of fluid parameter M on velocity profile. It is evident that by hiking the values of fluid parameter M the velocity profile enhances. Because, it is illustrated that by enhancing the M the density of the fluid particles reduces which causes increase in velocity. Figure 2a presents the impact of fluid parameter B on velocity. From this figure, decrease in velocity profile is noticed for increase values of fluid parameter B. Because, for increment in fluid parameter B, the viscosity of fluid particle enhances, and due to this
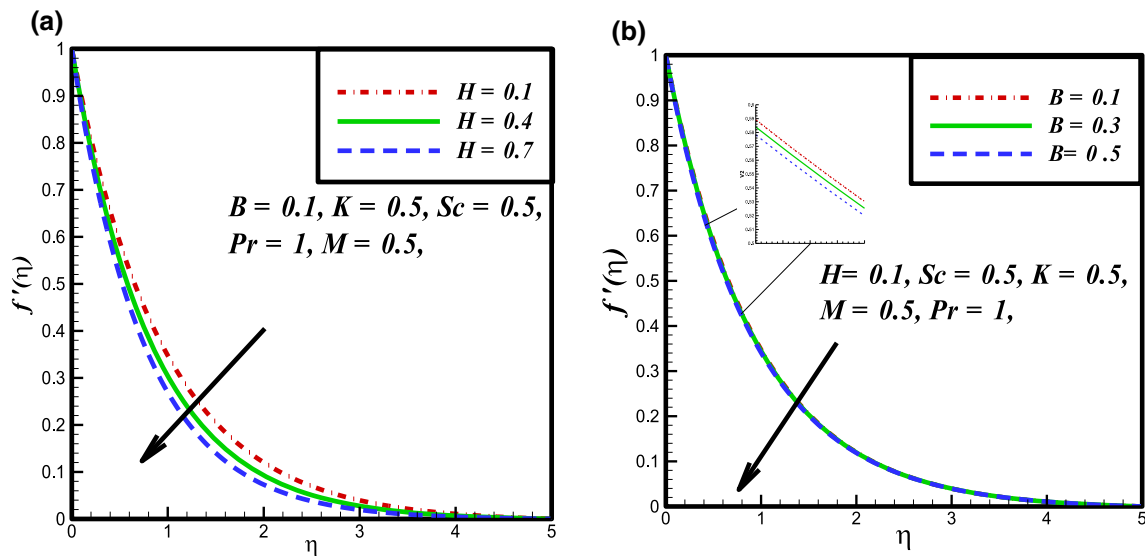
(a)

(b)

Fig. 1 Fluid velocity curves against **a** H and **b** fluctuations in B
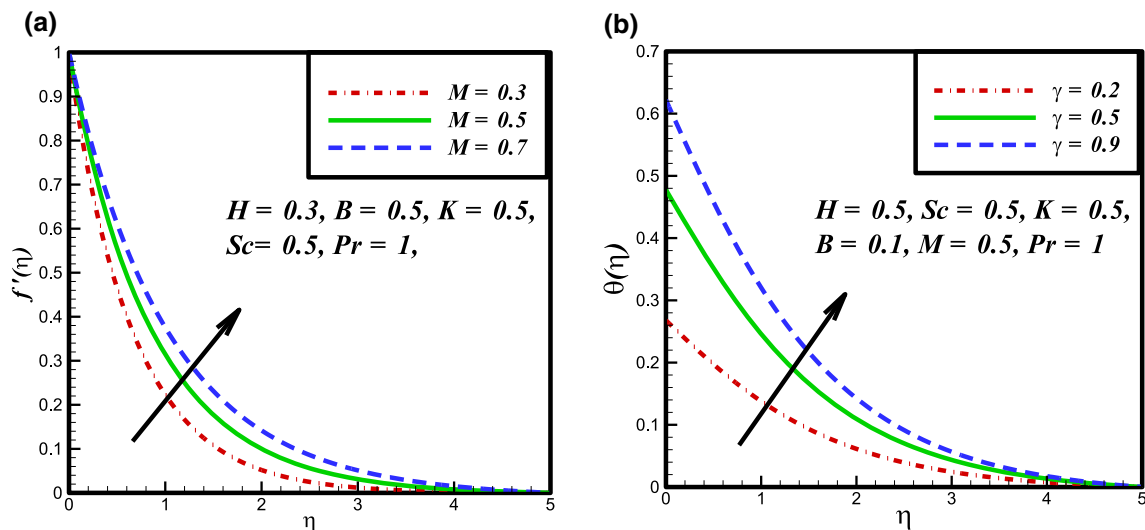
(a)

(b)

Fig. 2 a Fluid velocity curves against fluctuations in M, **b** Effect of γ on temperature profile

reason, the velocity profile reduces. Figure 2b shows the impact of Newtonian heating parameter γ on dimensionless temperature profile. As for Newtonian heating the value of conjugate parameter γ increase the thermal boundary layer thickness reduces eventually the temperature profile rise up. Figure 3a depicts the effect of Prandtl number Pr on dimensionless temperature profile. This figure reveals the reverse result for thermal boundary layer with increase in Prandtl number Pr when the thermal boundary layer falls down. The fluid has high conductivity for insignificant values of Prandtl number Pr. So by increasing the values of Prandtl number Pr, the thermal diffusivity reduces, which causes the decrease in temperature and thermal boundary layer of the fluid. Figures 3b and 4a show the effect of

homogenous and heterogeneous reactions parameter K and K_s on concentration profile. It is clear from this figure that thickness of concentration boundary layer enhances with η and after certain values of η it has no effect of concentration profile in both cases. Figure 4b represents the impacts of Schmidt number Sc on mass transfer rate. As the Schmidt number Sc is the diffusivity ratio, i.e., mass and momentum diffusivity, the mass diffusivity is small for large number of Schmidt number Sc due to this fact that the concentration profile enhances. Figure 5a shows the behavior of skin friction coefficient versus fluid parameter B and strength of magnetic parameter H. It is manifested from figure that skin friction enhances by increasing the fluid parameter B and Hartmann number H. Figure 5b
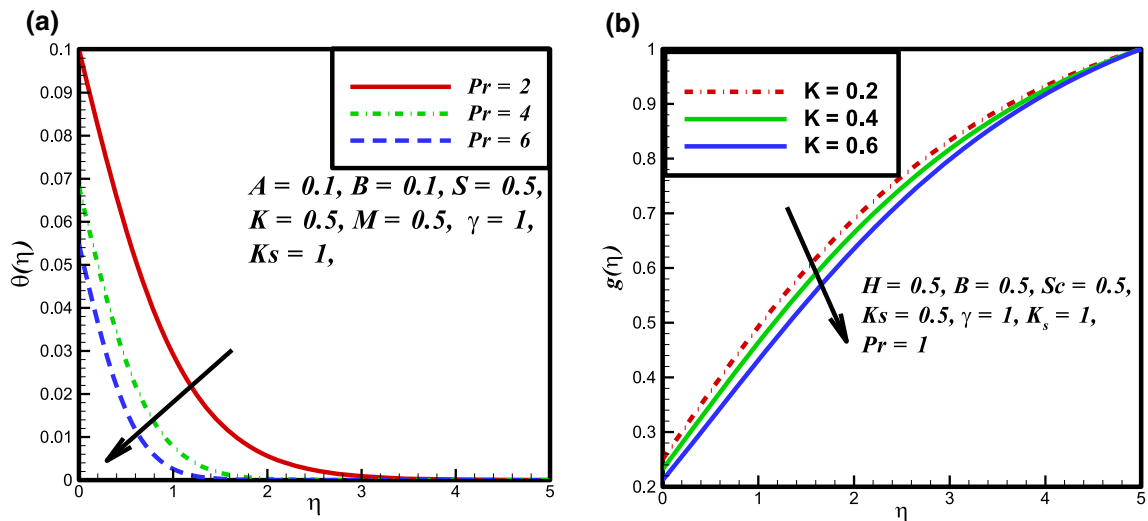
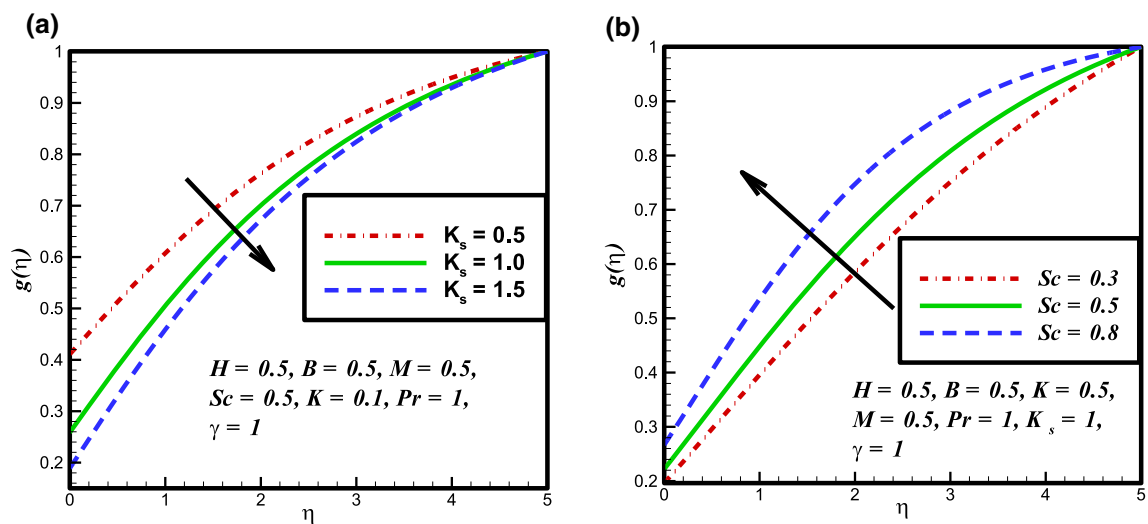**Fig. 3** Effect of **a** *Pr* on temperature profile and **b** *K* on concentration profile

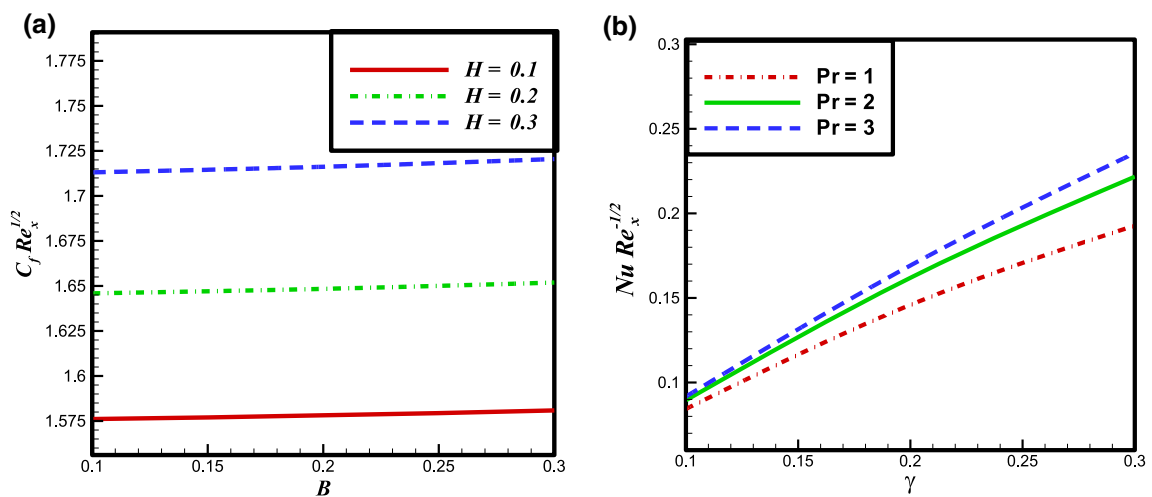**Fig. 4** Impact of **a** K_s and **b** *Sc* on concentration profile

Fig. 5 **a** Effect of *H* and *B* on skin friction coefficient, **b** effect of *Pr* and *γ* on Nusselt number

Table 1 Coefficient of skin friction against fluctuations in Hartmann number H and fluid parameters B and M

H	B	M	$C_f Re_x^{\frac{1}{2}}$
0.1	0.1	0.5	1.5761
0.2			1.6460
0.3			1.7131
0.1	0.1		1.5761
	0.2		1.5781
	0.3		1.5809
	0.5	0.5	1.5896
		0.6	1.5323
		0.7	1.4997

Table 2 Fluctuations in Nusselt number and Sherwood number against the parameters Pr, γ, Sc and K

Pr	γ	$NuRe_x^{-\frac{1}{2}}$
1	0.1	0.0844
3		0.0895
2		0.1692
1	0.1	0.0844
	0.2	0.1459
	0.3	0.1928

Sc	K	$ShRe_x^{-\frac{1}{2}}$
0.4	0.3	0.2250
0.6		0.2576
0.8		0.2900
0.4	0.3	0.2250
	0.4	0.2169
	0.5	0.2086

Table 3 Comparison of the present work for $f''(0)$ with Hartmann number H when $Sc = Pr = K = B = 0$ and $M = 0.0001$

H	Fang et al. [29]	Akbar et al. [1]	Salahuddin et al. [30]	This study
0		1	1	1
0.5		−1.11803	−1.11801	−1.11803
1		−1.41421	−1.41418	−1.41423
5		−2.44949	−2.44942	−2.44942
10		−3.31663	−3.31656	−3.31658
100	−1.1180	−10.04988	−10.04981	−10.04987
500		−22.38303	−22.38293	−22.38294
1000		−31.63859	−31.63846	−31.63846

Table 4 Comparison of the present work for $\theta'(0)$ with Pr when $Sc = K = Pr = 0$ and $M = 0.0001$

Pr	Wang [31]	Mabood et al. [31]	Salahuddin et al. [30]	This study
0.07	0.0656	0.0655	0.0654	0.0654
0.20	0.1691	0.1691	0.1688	0.1689
0.70	0.4539	0.4539	0.4534	0.4539
2.00	0.9114	0.9114	0.9108	0.9113
7.00	1.8954	1.8954	1.8944	1.8944
20.00	3.3539	3.3539	3.3522	3.3532
70.00	6.4622	6.4622	6.4619	6.4619

that by increasing the fluid parameter B and Hartmann number H skin friction increases, while it shows opposite behavior in the case of fluid parameter M. Table 2 describes the significance of different parameters on Sherwood number and Nusselt number. These parameters show increasing behavior in mass transfer coefficient for large digit of Prandtl number Pr and conjugate parameter of Newtonian heating γ. Concentration profile increases for large values of Schmidt number Sc and falls down for homogenous reaction parameter K. Tables 3 and 4 show the excellent correlation for the numerical values of $\theta'(0)$ and $f''(0)$ with previous results of the literature against variation of Hartmann number H and Prandtl number Pr.

3.1 Concluding remarks

The study of two-dimensional homogenous and heterogeneous reactions in Powell–Eyring fluid model is considered numerically under the influence of MHD and Newtonian heating. The main results of this problem are:

1. A substantial reduction in the fluid parameters B and Hartmann number H was noticed in velocity profile.
2. A qualitatively opposite behavior was analyzed in the velocity profile for increasing values of for Newtonian heating parameter γ and Prandtl number Pr.
3. Concentration profile reduced by increasing homogenous and heterogeneous reactions parameter K and K_s, but showed opposite behavior for Schmidt number Sc.
4. Skin friction coefficient enhanced when Hartmann number H and fluids parameters B and M increased.
5. Concentration profile enhanced for large values of homogenous reaction parameter K, heterogeneous reaction parameter K_s and Schmidt number Sc.

shows the effect of Prandtl number Pr and γ on Nusselt number. It is analyzed that for Newtonian heating the conjugate parameter γ reduces but Prandtl number Pr increase the Nusselt number. Table 1 shows the result of different parameters in skin friction coefficient. It is found

References

1. Akbar NS, Ebaid A, Khan ZH (2015) Numerical analysis of magnetic field effects on Powell–Eyring fluid flow towards a stretching sheet. J Magn Magn Mater 382:355–358

2. Malik MY, Hussain A, Nadeem S (2013) Boundary layer flow of an Powell–Eyring model fluid due to a stretching cylinder with variable viscosity. Sci Iran 20:313–321

3. Ara A, Khan NA, Khan H, Sultan F (2014) Radiation effect on boundary layer flow of an Powell–Eyring fluid over an exponentially shrinking sheet. Ain Shams Eng J 5:1337–1342

4. Nadeem S, Saleem S (2014) Mixed convection flow of Powell–Eyring fluid along a rotating cone. Results Phys 4:54–62

5. Hayat T, Ali S, Farooq MA, Alsaedi A (2015) On Comparison of series and numerical solutions for flow of Eyring-Powell fluid with Newtonian heating and internal heat generation/absorption. PLOS One. doi:10.1371/journal.pone.0129613

6. Malik MY, Salahuddin T, Hussain A, Bilal S (2015) MHD flow of tangent hyperbolic fluid over a stretching cylinder: using Keller box method. J Magn Magn Mater 395:271–276

7. Malik MY, Khan I, Hussain A, Salahuddin T (2015) Mixed convection flow of MHD Powell–Eyring nanofluid over a stretching sheet: a numerical study. AIP Adv 5:117–121

8. Nawaz M, Zeeshan A, Ellahi R, Abbasbandy S, Rashidi S (2015) Joules heating effects on stagnation point flow over a stretching cylinder by means of genetic algorithm and Nelder-Mead method. Int J Numer Methods Heat Fluid Flow 25:665–684

9. Rosca AV, Pop I (2014) Flow and heat transfer of Powell–Eyring fluid over a shrinking surface in a parallel free stream. Int J Heat Mass Transf 71:321–327

10. Salahuddin T, Malik MY, Hussain A, Bilal S, Awais M (2015) Effects of transverse magnetic field with variable thermal conductivity on tangent hyperbolic fluid with exponentially varying viscosity. AIP Adv 5:127103

11. Merkin JH (1996) A model for isothermal homogeneous-heterogeneous reactions in boundary-layer flow. Math Comput Model 24:125–136

12. Sarif NM, Salleh MZ, Nazar R (2013) Numerical Solution of flow and heat transfer over a stretching sheet with Newtonian heating using the Keller box method. Procedia Eng 53:542–554

13. Kameswaran K, Shaw S, Siband P, Murthy PVS (2013) Homogeneous heterogeneous reactions in a nanofluid flow due to a porous stretching sheet. Int J Heat Mass Transf 57:465–472

14. Shaw S, Kameswaran PK, Sibanda P (2013) Homogeneous-heterogeneous reactions in micropolar fluid flow from a permeable stretching or shrinking sheet in a porous medium. Bound Value Probl. doi:10.1186/1687-2770-2013-77

15. Abbas Z, Sheikh M, Pop I (2015) Stagnation-point flow of a hydromagnetic viscous fluid over stretching/shrinking sheet with generalized slip condition in the presence of homogeneous–heterogeneous reactions. J Taiwan Inst Chem Eng 55:1–7

16. Ellahi R, Zeeshan A, Hassan M (2015) Shape effects of mixed convection MHD nanofluid over a vertical stretching permeable sheet. J Zhejiang Univ Sci A. doi:10.1631/jzus.A1500119

17. Labropulu F, Li D, Pop I (2010) Non-orthogonal stagnation-point flow towards a stretching surface in a non-Newtonian fluid with heat transfer. Int J Therm Sci 49:1042–1050

18. Salahuddin T, Malik MY, Hussain A, Bilal S, Awais M (2016) MHD flow of Cattanneo-Christov heat flux model for Williamson fluid over a stretching sheet with variable thickness: using numerical approach. J Magn Magn Mater 401:991–997

19. Nadeem S, Hussain A, Khan M (2010) HAM solutions for boundary layer flow in the region of the stagnation point towards a stretching sheet. Commun Nonlinear Sci Numer Simul 15:475–481

20. Nadeem S, Zaheer S, Fang T (2011) Effects of thermal radiation on the boundary layer flow of a Jeffrey fluid over an exponentially stretching surface. Numer Algorithms 57:187–205

21. Akbar NS, Nadeem S, Haq RL, Khan ZH (2013) Numerical solutions of magnetohydrodynamic boundary layer flow of tangent hyperbolic fluid towards a stretching sheet. Indian J Phys 87:1121–1124

22. Malik MY, Naseer M, Nadeem S, Rehman A (2014) The boundary layer flow of Casson nanofluid over a vertical exponentially stretching cylinder. Appl Nanosci 4:869–873

23. Tian XY, Li BW, Wu YS, Zhang JK (2015) Chebyshev collocation spectral method simulation for the 2D boundary layer flow and heat transfer in variable viscosity MHD fluid over a stretching plate. Int J Heat Mass Transf 89:829–837

24. Lee JH (2015) Turbulent boundary layer flow with a step change from smooth to rough surface. Int J Heat Fluid Flow 54:39–54

25. Zeeshan A, Majeed A, Ellahi R (2016) Effect of magnetic dipole on viscous ferro-fluid past a stretching surface with thermal radiation. J Mol Liq 215:549–554

26. Majeed A, Zeeshan A, Ellahi R (2016) Unsteady ferromagnetic liquid flow and heat transfer analysis over a stretching sheet with the effect of dipole and prescribed heat flux. J Mol Liq 223:528–533

27. Maqbool K, Sohail A, Manzoor N, Ellahi R (2016) Hall effect on Falkner—Skan boundary layer flow of FENE-P fluid over a stretching sheet. Commun Theor Phys 66:547–554

28. Alsaedi A, Alsaadi FE, Ali S, Hayat T (2013) Stagnation point flow of Burgers' fluid and mass transfer with chemical reaction and porosity. J Mech. doi:10.1017/jmech.2013.20

29. Fang T, Zhang J, Shanshan Y (2009) Slip MHD viscous flow over a stretching sheet an exact solution. Commun Nonlinear Sci Numer Simul 14:3731–3737

30. Wang CY (1989) Free convection on a vertical stretching surface with suction and blowing. Appl Math Mech 69:418–420

31. Mabood F, Khan WA, Ismail AIM (2015) MHD boundary layer flow and heat transfer of nanofluids over a nonlinear stretching sheet: a numerical study. J Magn Magn Mater 374:569–576